

Western University

Scholarship@Western

---

Electrical and Computer Engineering  
Publications

Electrical and Computer Engineering  
Department

---

Fall 10-1-2018

## Development of MR Clutch for a Prospective 5-DOF Robot

Sergey Pisetskiy

*The University of Western Ontario*

Mehrdad Kermani Ph.D., P.Eng.

*Western University, mkermani@eng.uwo.ca*

Follow this and additional works at: <https://ir.lib.uwo.ca/electricalpub>



Part of the [Computer Engineering Commons](#), and the [Electrical and Computer Engineering Commons](#)

---

### Citation of this paper:

Pisetskiy, Sergey and Kermani, Mehrdad Ph.D., P.Eng., "Development of MR Clutch for a Prospective 5-DOF Robot" (2018). *Electrical and Computer Engineering Publications*. 557.

<https://ir.lib.uwo.ca/electricalpub/557>

# Development of MR Clutch for a Prospective 5 DOF Robot\*

Sergey Pisetskiy and Mehrdad R. Kermani<sup>1</sup>

**Abstract**—This paper presents an improved design approach for the construction of a Magneto-Rheological (MR) clutch intended to be used in a prospective 5 degrees of freedom robot. The MR clutch features embedded Hall sensors for intrinsic torque control. After a brief description of the MR clutch principles, the details of the mechanical design are discussed. Simulation and preliminary experimental results demonstrate the main characteristics and advantages of the proposed MR clutch.

## I. INTRODUCTION

There is increasing attention focused on the use of magneto-rheological clutches and brakes due to their unique characteristics such as high torque to weight ratio, low power consumption, high operating speed, and precision in torque control. Several companies have begun to use MR clutches in their commercial products such as knee prosthesis [1] and Steer-by-Wire system for mobile equipment [2]. More companies actively study the feasibility of implementing new MR technologies to replace or enhance existing solutions such as transmission system clutches for automotive and power equipment [3], [4], cooling systems [5], agricultural metering systems [6], and haptic control systems for airborne vehicles [7].

Rehabilitation equipment [8], exoskeletons [9], and collaborative robots [10], [11] are also emerging areas that can benefit from MR technology implementation. These applications entail new requirements for a balanced approach for achieving compliant and safe interactions with humans and the environment while maintaining the desired level of performance of the robot.

In this paper we present an improved design for the construction of an MR clutch increasing torque-to-mass ratio and torque resolution. The device has been developed to be integrated into an interactive robot using Distributed Active Semi-Active approach [12].

The contributions of this work are as follows:

- An innovative design of an MR clutch with the high torque-to-mass ratio is described.
- A new arrangement of the Hall sensors inside the MR clutch is proposed.
- Preliminary experimental results are presented to validate the proposed design while highlighting the new clutch torque capabilities.

\*This work was supported in part by Canada Foundation for Innovation (CFI) and Natural Sciences and Engineering Research Council (NSERC) of Canada under grant No.25031 and RGPIN-346166.

<sup>1</sup>The authors are with the Electrical and Computer Engineering Department, the University of Western Ontario, London, ON N6A 5B9 Canada [spisetsk@uwo.ca](mailto:spisetsk@uwo.ca), [mkermani@eng.uwo.ca](mailto:mkermani@eng.uwo.ca)

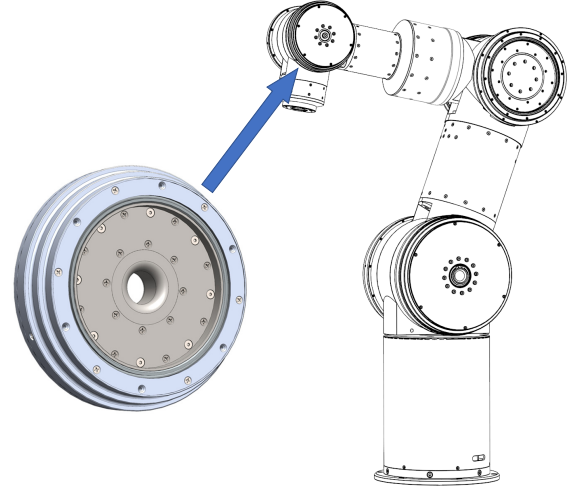


Fig. 1. Prospective 5 DOF Robot and location of the MR clutch in the 5<sup>th</sup> joint.

## II. OVERVIEW

MR clutches are unique devices that not only provide intrinsic compliance for safe actuation but also lend themselves to a new actuation concept in robotic systems. By controlling the viscosity of MR fluids (from liquid to near solid) using an internal magnetic field, accurate transmission of provided torque to the robot link using an MR clutch (i.e., a Semi-Active system) is controlled. As an alternative configuration, a pair of MR clutches can drive a load antagonistically similar to human muscle actuation [12], [10]. This actuation concept gives rise to a new design framework in which a single active source (motor) can drive multiple loads using multiple MR clutches simultaneously and independently [13], [14]. This new framework, termed DASA (Distributed Active Semi-Active Actuation), results in systems that are lightweight, cost-effective, compliant, and safe [15]. The complete analysis of DASA has been previously reported to provide a guideline for selecting suitable configurations and parameters of MR actuation for various applications [16], [17]. Hybrid magnetization using a combination of permanent magnets and electric coils was developed to further reduce weight and enhance actuation bandwidth (speed) [18]. A force/torque control algorithm with high fidelity was developed using a new hysteresis model [19].

### A. Design Objectives

The main objective of the current work is to develop an MR clutch with enhanced capabilities for the 5<sup>th</sup> joint of the

prospective 5-DOF robot manipulator. Fig.1 shows a possible mechatronic layout for a manipulator and location of the magneto-rheological clutch.

The targeted payload for the manipulator is 10 kg at full extension of the robotic arm. Given its long reach, the manipulator has much higher payload inside the boundary of its workspace. Each joint of the manipulator is actuated using a pair of MR clutches coupled in an antagonistic configuration. The manipulator in total includes 10 MR clutches with maximum direct torque delivered to their corresponding joints without gear reduction. The required torque values for each joint are listed in Table I.

TABLE I  
REQUIRED TORQUES OF MR CLUTCHES AT THE ROBOT JOINTS

Joint	1	2	3	4	5
Torque [Nm]	15	200	80	15	15

### B. Working Principles of MR clutches

An MR clutch is the building block of the proposed robot manipulator. The function of the MR clutch is mainly the continual transmission of the actuation torque from the motor side to the load side. By changing the viscosity of the MR fluid, the exact amount of transmission torque is regulated. The viscosity of MR fluid can be precisely controlled by applying a magnetic field in accordance with the requirement of load transfer. The principle operation of a single-disk MR clutch is shown in Fig. 2.

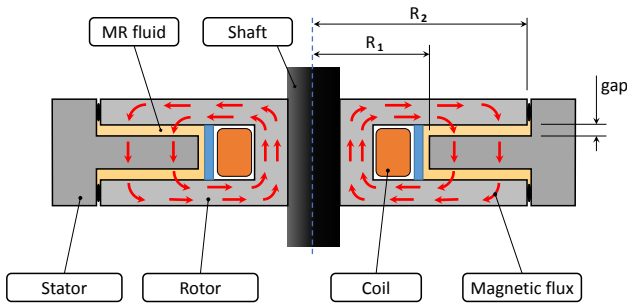


Fig. 2. Cross-section view of a single-disk MR clutch.

As seen, the rotor of the clutch made of ferromagnetic materials along with the electromagnetic coil is mounted on the input shaft of the clutch. The input shaft can be powered by any type of electric motor (i.e., DC, AC, synchronous, or asynchronous) to provide free rotation relative to the stator. The stator in this clutch consists of a single ferromagnetic disc. In general, the stator can include as many discs as required for a nominal torque capacity. The gap between the stator disc and the rotor is filled with MR fluid. The magnetic field generated by the coil increases the yield strength in the directions perpendicular to the magnetic flux. The resulting shear stress over the whole surface of the disc transmits the

limited amount of torque from the input shaft and rotor to the output stator.

The roles of rotor and stator can be easily swapped in an MR clutch without the need for any modification to the clutch itself. In other words, the outer part of the clutch and the disc can act as the rotor and be powered by an external motor to rotate continuously, while the shaft and the inner part of the clutch can be used as the stator to transmit torque to the load. The electromagnetic coil can be mounted on either stator or rotor. If the electromagnetic coil is mounted on the rotor, a slip ring mechanism is required to provide electrical connection.

A pair of MR clutches can be configured to provide antagonistic actuation to a load. In this case, the rotors of the MR clutches are rotated in opposite directions and the stators of both MR clutches are coupled to a common shaft. Depending on the electromagnetic activation of each clutch, the torque can be applied by one or both MR clutches in either direction.

A complete comparison of various MR clutch configurations can be found in [20], [21], [16].

### III. IMPROVED DESIGN OF THE MR CLUTCH

In order to develop a lightweight, strong, and reliable actuator, various types of MR clutches including drum-type, multi-drum, multi-disk, and drum-disk hybrid MR clutches were considered [16]. Given the characteristics of each type and our design requirements for performance and manufacturability, a multi-disk MR clutch with hybrid magnetization configuration was identified to best meet our design requirements.

In the following, the details of the selected MR clutch configuration for the 5<sup>th</sup> joint of the robot manipulator are described. A similar MR clutch configuration is used for all other joints of the robot.

The selected design of the MR clutch follows the conventional configuration of multi-disk MR clutches. As shown in Fig. 3, the stationary part of the MR clutch, i.e., the stator, comprises a carbon steel core, an electromagnetic coil, a permanent magnet, and four carbon steel disks separated by aluminum spacers at the inner diameter.

The rotor, the moving part of the MR clutch, consists of five carbon steel disks that are arranged in between the stator disks. Aluminum spacers at the outer diameter keep the rotor disks separated from each other. The aluminum spacers of the rotor and the stator ensure a consistent gap size (of 0.4 mm) between the stator and rotor disks. The gaps are filled with MR fluid that is injected through fill/drain ports on the rotor side. Dynamic seals prevent the fluid from escaping the volume between the disks (active zone). The MR clutch also includes Hall sensors to provide feedback of the internal magnetic field, and subsequently, the generated torque of the MR clutch.

What sets the proposed design apart from the conventional multi-disk MR clutches is the location and arrangement of the Hall sensors. Unlike conventional MR clutches [18], [14], the Hall sensors (two Infineon TLE 4998s4 programmable

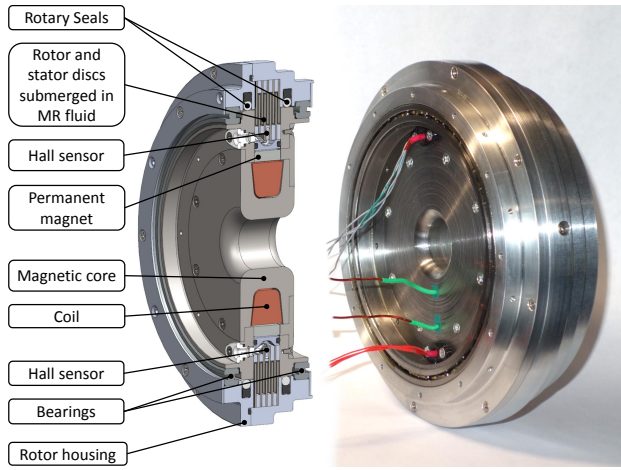


Fig. 3. Section view of the 5<sup>th</sup> joint MR clutch.

sensors) are located within a cut in an aluminum spacer outside the active zone of the MR clutch. By placing the Hall sensor outside the active zone as shown in Fig. 4, a small fraction of the magnetic field strength with respect to conventional placement of the Hall sensors is used for measurement and providing feedback.

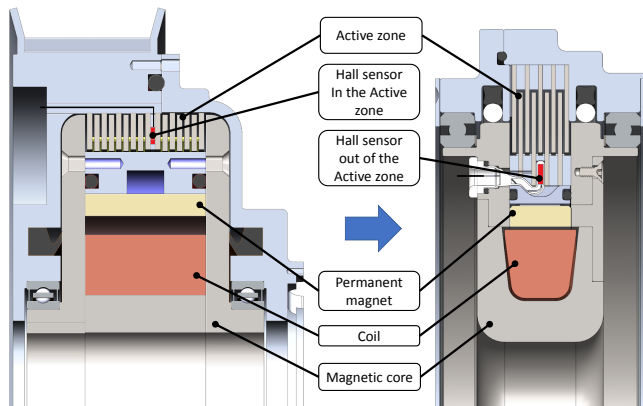


Fig. 4. Comparison of the conventional Hall sensor location (left) with the proposed location outside of the MR clutch active zone (right).

The advantages of the proposed location are multifold. First, by placing the Hall sensor, not within the active zone between a stator and rotor disk, the gap between these disks can be dramatically reduced, thereby reducing the total reluctance of the magnetic circuit and increasing the generated torque of the clutch for a given input current. Second, the space dedicated for housing the Hall sensors within a sandwiched aluminum disk between a stator and rotor disk can be used for an additional rotor disk, contributing to a higher nominal torque value of the MR clutch (see Fig. 5, 6, and 7). Finally, by placing the Hall sensor outside of the active zone, a small fraction of the magnetic field is used for measurement which provides higher torque resolution given the limited maximum reading capacity of the sensor. These changes due to the new location of the Hall Sensor substantially improve the performance of the MR clutch also

in terms of power-to-weight ratio and energy consumption.

In order to improve connection reliability and further reduce assembly encumbrance, both Hall sensors and the electromagnetic coil are designed to be located on the stationary core of the stator to avoid the disadvantages of the slip-ring mechanism.

#### IV. SIMULATION AND OPTIMIZATION

The geometry of the proposed MR clutch was carefully optimized using Finite Element Method (FEM) in COMSOL Multiphysics software. Fig. 5, 6, 8, and 10 show the map of the magnetic flux density at the various current densities and the magnetic field of the permanent magnet. Based on the color distribution, the geometry of the clutch is adjusted to create a uniform distribution of the flux lines and to avoid saturation in the local areas of the magnetic circuit as much as possible.

Fig. 5 shows the map of the magnetic flux density for the conventional design of MR clutch with the Hall sensor located in the active zone between two stator discs as in [18]. Fig. 6 shows the magnetic flux distribution in the proposed design, where the sensor is positioned outside the active zone. Both maps are generated for the magnet wire current 2 A (total coil current 300 A for 150 turns of wire).

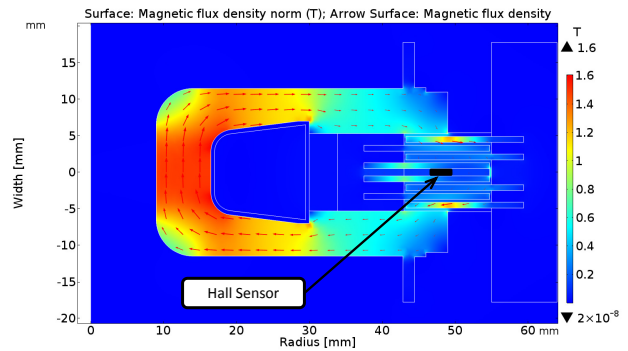


Fig. 5. MR clutch Magnetic flux density contour map in the conventional design with Hall sensor in the active zone (wire current 2 A, total coil current 300 A).

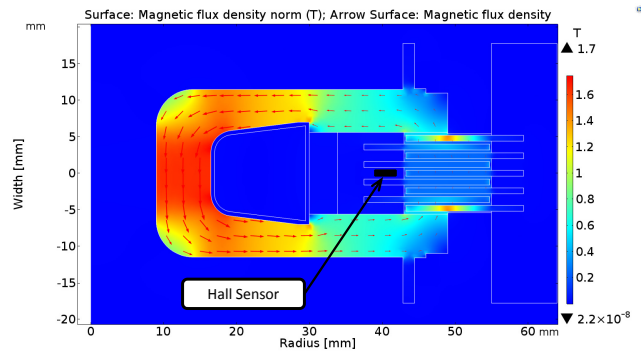


Fig. 6. MR clutch Magnetic flux density contour map in the proposed design with Hall sensor outside the active zone (wire current 2 A, total coil current 300 A).

As a result of moving the Hall sensors out of the active zone, the proposed MR clutch provides 1.68 times higher

transmitted torque at 1 A, 1.48 times at 2 A, and 1.42 at 3 A wire current as is shown on the Fig. 7.

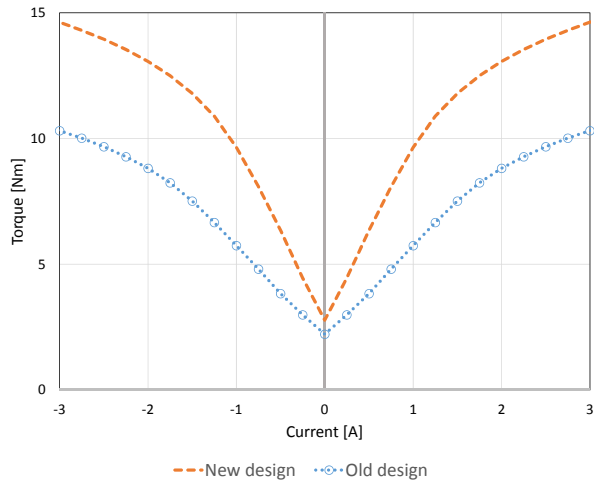


Fig. 7. The relation between the current in the winding (A) and transmitted torque (N·m) for the old design (Hall sensors in the active zone) and for the new design (Hall sensors outside the active zone).

Fig. 8 displays the map of the magnetic flux density for the proposed design of MR clutch with the permanent magnet ( $B = 1.35$  T) mounted around the coil as shown in Fig. 3 (wire current 2 A, the total coil current 300 A). It can be observed that the density of the flux in the central part of the magnetic core is significantly reduced, while the density in the active zone is increased in comparison with the clutch with no permanent magnet inserted (Fig. 6).

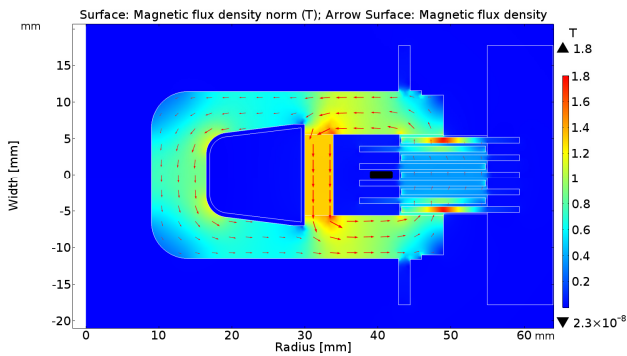


Fig. 8. MR clutch Magnetic flux density contour map at the coil wire current 2 A (wire current 2 A, total coil current 300 A) with permanent magnet inserted ( $B = 1.35$  T).

Fig. 9 shows the relationships between the current in the winding and the transmitted torque for the proposed MR clutch with no permanent magnet ( $B_{mag} = 0$ ), with a weak magnet ( $B_{mag} = 0.5$  T), and with a strong permanent magnet ( $B_{mag} = 1.35$  T). It can be observed that the maximum transmitted torque increases with the strength of the permanent magnet used. The maximum torque of 13.5 N·m, 21.3 N·m, and 26.9 N·m can be transmitted at wire current 1 A, 2 A, and 3 A respectively (the total coil current 150 A, 300 A, and 450 A for 150 turns of magnet wire).

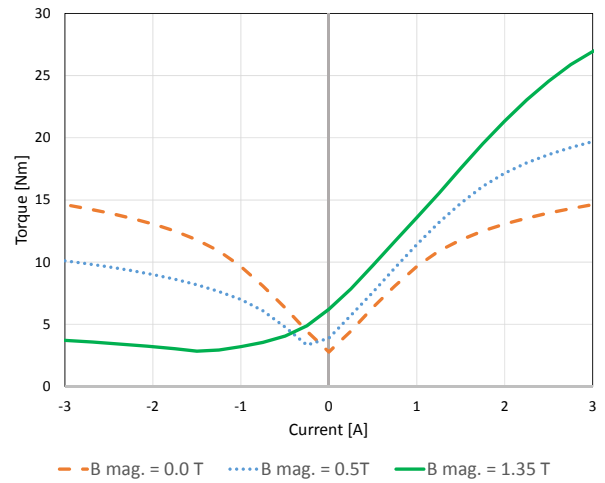


Fig. 9. The relation between the current in the winding (A) and transmitted torque (N·m).

Taking into account the mass of the MR clutch (1.8 kg), the torque to mass ratios for the 1 A, 2 A, and 3 A wire current can be estimated as 7.5 N·m/kg, 11.8 N·m/kg, and 14.9 N·m/kg respectively.

In order to further increase the torque to mass ratio, the configuration with the reduced gap size (from 0.4 mm to 0.2 mm) is developed and evaluated in COMSOL Multiphysics. In the new configuration the thickness of the rotor and stator disks is reduced from 0.8 mm to 0.4 mm; the number of disks for the rotor is 9 and the number of disks for the stator is 8. The thickness of the central rotor disk is 1.18 mm in order to locate the Hall sensor between two stator disks. Fig. 10 displays the map of the magnetic flux density for the proposed 0.2 mm gap design of MR clutch with the permanent magnet ( $B = 1.35$  T, wire current 2 A, the total coil current 300 A).

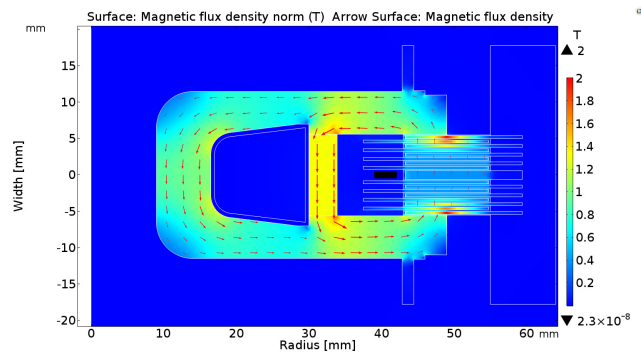


Fig. 10. 0.2 mm gap MR clutch Magnetic flux density contour map at the coil wire current 2 A (wire current 2 A, total coil current 300 A) with permanent magnet inserted ( $B = 1.35$  T).

Fig. 11 shows the relation between the current in the winding and the transmitted torque for the 0.2 mm gap and 0.4 mm gap MR clutches with permanent magnet ( $B_{mag} = 1.35$  T) inserted.

It can be observed that the transmitted torque of the 0.2 mm gap clutch reaches values of 25.7 N·m, 40.4 N·m, and

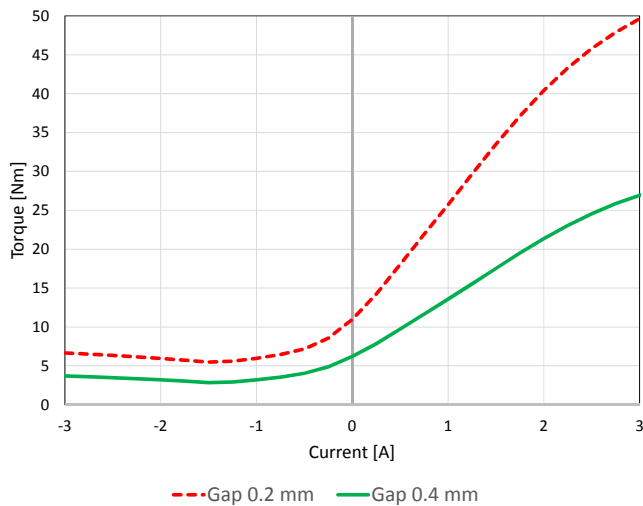


Fig. 11. The relation between the current in the winding (A) and transmitted torque (N·m) for 0.2 mm and 0.4 mm gap MR clutches.

49.6 N·m for wire current 1 A, 2 A, and 3 A respectively. The torque to mass ratios can be estimated as 14.2 N·m/kg, 22.4 N·m/kg, and 27.5 N·m/kg respectively.

## V. PRELIMINARY EXPERIMENTAL RESULTS

In order to validate the capability of the proposed design to transmit the required torque, a prototype MR clutch with 0.4 mm gap size was built. The MR clutch was tested under various load conditions and the obtained experimental data were compared with the corresponding simulated values.

To perform the experiments, the part of the 5 DOF robot base with the motor and the HD gearbox was assembled. The base was equipped with a frame to mount a static load cell (Transducer Techniques SBO-1K) as shown in Fig. 12. An adapter on the top of the clutch was used to firmly couple the stator to the load cell. A similar adapter underneath the MR clutch was used to transmit the rotational input from the HD gearbox to the clutch rotor.

As previously mentioned, the prospective 5-DOF robot (and all MR clutches) will be powered using a single 2800 watt DC motor (Hacker Q80-13XS). For the purpose of the experiments, a simple motor driver (Advanced Motion Control AZ12A8) was also used to supply current to the electromagnetic coil of the MR clutch. An interface box (Infineon PGSISI-2 board) was used to read the data provided by the Hall sensors. The entire setup was controlled using a real-time controller board (dSPACE DS 1103) to run the motor at a constant speed, to provide (current) command signals for the MR clutches through the motor driver, and to acquire feedback data from the load cell and Hall sensors.

In an initial test, a sinusoidal current with the frequency of 1 Hz and an amplitude of  $\pm 2.5$ A was used to drive the electromagnetic coil of the prototype MR clutch while the output torque of the clutch was measured. Fig. 13 shows the measured torque values versus the input current of the MR clutch (blue solid line) and compares these results with

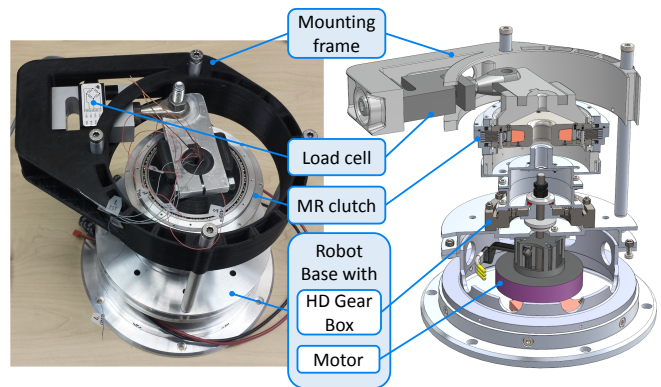


Fig. 12. Experimental setup with the 5th joint clutch installed.

their corresponding simulated values obtained in COMSOL Multiphysics (orange dash line).

The graphs illustrate a clear agreement between the modeled and the actual measured data. The main discrepancies between the data occur at the lower end of the input current (less than  $\pm 0.3$  A) where the COMSOL FEM model cannot reflect the effect of magnetic hysteresis within the materials as seen in experimental data.

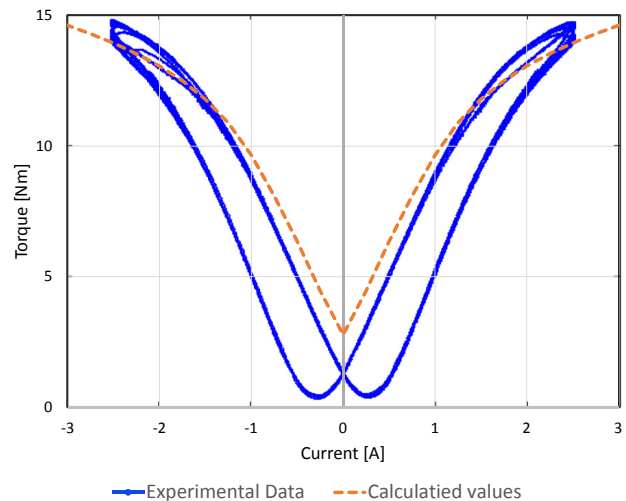


Fig. 13. Experimental and simulated results for the MR clutches used in the 5<sup>th</sup> joint: the relation between the current in the winding (A) and transmitted torque (N·m).

A subsequent test validated the feasibility of the proposed placing of the Hall sensors outside the active zone of the MR clutch. To this end, multiple continuous currents with different magnitude ranging from -3A to 4.5A were applied to the magnetic coil of the MR clutch and the corresponding magnetic flux intensities read by the Hall sensors were recorded. The data was compared with the one obtained using simulation. Fig. 14 compares the experimental (solid blue) and simulated (dashed orange) results. The good match between the results validates the proposed Hall sensor arrangement for the MR clutches.

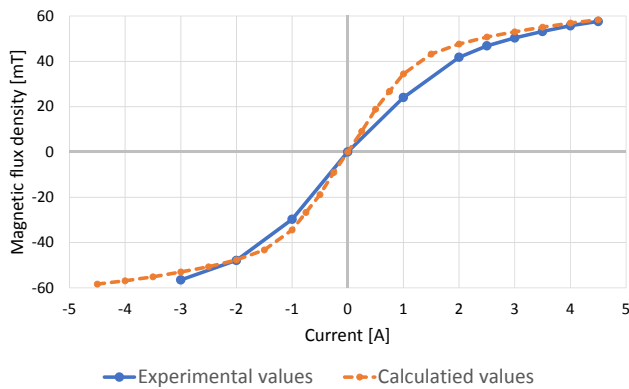


Fig. 14. Experimental and simulated magnetic flux densities for the 5<sup>th</sup> joint MR clutches. The Relation between the current in the winding (A) and Hall sensor reading (mT).

## VI. CONCLUSION

An improved design of a magneto-rheological clutch is presented in this paper to demonstrate the possibility of building an MR actuator with enhanced performance.

The relocation of Hall sensors out of the active area, implementation of a strong permanent magnet, and fine-tuning of the geometry of the magnetic core, resulted in 11.8 N-m/kg torque to mass ratio for the clutch (3.2 Watt power consumption). The reduction of the gap size between the discs from 0.4 mm to 0.2 mm along with increasing the total number of disks from 9 to 17 helped to further improve the torque to mass ratio, estimated as 22.4 N-m/kg with the same power consumption.

Preliminary tests of the first built prototype, described in the paper, confirm the performance of the clutch with 0.4 mm gap size. Presented results show good correlation between the developed COMSOL model and the actual hardware. According to the tests performed, the Hall sensors mounted in the proposed location can be successfully used to estimate the magnetic flux in the active area.

The drawbacks of the developed design are as follows:

- increased friction torque at the joint due to MR fluid viscosity in the decreased gaps between the disks;
- additional power required to cancel the permanent magnet in order to keep the clutch disengaged;
- increased wear of parts caused by stronger interaction forces;
- changes in the hysteresis pattern that can "annoy" the controller.

Further work is in progress to fabricate and test a 0.2 mm gap MR clutch, dynamical test, and study the hysteresis behavior of the clutch.

## REFERENCES

- [1] <https://www.ossur.com/prosthetic-solutions/products/dynamic-solutions/rheo-knee>.
- [2] LORD TFD<sup>®</sup> Steering Units - Overview, [http://www.lordmrstore.com/\\_literature\\_240878/LORD\\_TFD\\_Steering\\_Units\\_-\\_Overview](http://www.lordmrstore.com/_literature_240878/LORD_TFD_Steering_Units_-_Overview)
- [3] C. Kieburg, "MR all-wheel-drive prototype car driving tests and durability requirements for the MR fluids used," in *Proceedings of ERM08*, 2008.
- [4] A. J. McDaniel, "Magneto-rheological brake-clutch apparatuses and methods," Apr. 29 2008, US Patent 12,111,578.
- [5] A.L. Smith, J.C. Ulicny, and L.C. Kennedy, "Magneto-rheological fluid fan drive for trucks," *Journal of Intelligent Material Systems and Structures*, 18:1131-1136, 2007.
- [6] J. W. Henry, S. D. Noble, "Agricultural metering system having a magneto-rheological fluid clutch assembly," Aug. 31 2015, US Patent 14,841,427.
- [7] G. C. Lantham, C. A. Fenny, J. S. Plane, B. Atkins, G. Julio, M. Denninger, C. E. Covington, P. Wilson, "Magneto-rheological haptic trim actuator," Jan. 01 2014, US Patent 96,567,46B2.
- [8] T. Kikuchi, K. Oda, J. Furusho, "Development of Leg-Robot for Simulation of Spastic Movement with Compact MR Fluid Clutch," in *Robotics and Automation (ICRA), 2009 IEEE International Conference on*, IEEE, 2009, pp. 1903-1908.
- [9] M. Okui, S. Iikawa, Y. Yamada, T. Nakamura, "Variable Viscoelastic Joint System and Its Application to Exoskeleton," *Intelligent Robots and Systems (IROS), 2017 IEEE/RSJ International Conference on*, 2017, pp. 3897-3902.
- [10] P. Fauteux, M. Lauria, B. Heintz, and F. Michaud, "Dual-differential rheological actuator for high-performance physical robotic interaction," *Robotics, IEEE Transactions on*, vol. 26, no. 4, 2010, pp. 607-618.
- [11] J. Viau et al., "Projected PID controller for Tendon-Driven Manipulators actuated by magneto-rheological clutches," in *Intelligent Robots and Systems (IROS), 2015 IEEE/RSJ International Conference on*, 2015, pp. 5954-5959.
- [12] A. S. Shafer and M. R. Kermani, "On the feasibility and suitability of MR fluid clutches in human-friendly manipulators," *Mechatronics, IEEE/ASME Transactions on*, vol. 16, no. 6, 2011, pp. 1073-1082.
- [13] M. R. Kermani and A. Shafer, "Magneto- and electro-rheological based actuators for human friendly manipulators," Sep. 30, 2014, US Patent 20 150 107 395.
- [14] A. Shafer and M. R. Kermani, "Magneto-rheological clutch with sensors measuring electromagnetic field strength," Feb. 28 2013, US Patent 20,130,047,772.
- [15] A. S. Shafer and M. R. Kermani, "Development of high performance intrinsically safe 3-DOF robot," in *Robotics and Automation (ICRA), 2014 IEEE International Conference on*. IEEE, 2014, pp. 619-624.
- [16] W. Li, P. Yadmellat, and M. R. Kermani, "Design optimization and comparison of magneto-rheological actuators," in *Robotics and Automation (ICRA), 2014 IEEE International Conference on*. IEEE, 2014, pp. 5050-5055.
- [17] N. Najmaei, A. Asadian, M. R. Kermani and R.V. Patel "Design and Performance Evaluation of a Prototype MRF-Based Haptic Interface for Medical Applications," in *Mechatronics, IEEE/ASME Transactions on*, vol. 21, no. 1, 2016, pp.110-121.
- [18] M. Moghani and M. R. Kermani, "Design and development of a hybrid Magneto-Rheological clutch for safe robotic applications," in *Robotics and Automation (ICRA), 2016 IEEE International Conference on*. IEEE, 2016, pp. 3083-3088.
- [19] P. Yadmellat and M. R. Kermani, "Adaptive modeling of a magneto-rheological clutch," *Mechatronics, IEEE/ASME Transactions on*, vol. 19 IEEE, 2014, pp. 1716-1723.
- [20] Q. Nguyen and S. Choi, "Optimal design of a novel hybrid mr brake for motorcycles considering axial and radial magnetic flux," *Smart Materials and Structures*, vol. 21, no. 5, p. 055003, 2012.
- [21] Q. Nguyen and S. Choi, "Selection of magneto-rheological brake types via optimal design considering maximum torque and constrained volume," *Smart Materials and Structures*, vol. 21, no. 1, p. 015012, 2012.
- [22] K. D. Weiss and J. D. Carlson, "A growing attraction to magnetic fluids," *Machine design*, vol. 66, no. 15, 1994, pp. 61-64.
- [23] R. W. Phillips, "Engineering applications of fluids with a variable yield stress," Ph.D. dissertation, University of California, Berkeley, 1969.
- [24] T. Kikuchi, K. Otsuki et al., "Development of a Compact Magneto-rheological Fluid Clutch for Human-Friendly Actuator," *Advanced Robotics*, 24:10., 2010, pp. 1489-1502.
- [25] Lord Technical Data, MRF-140CG Magneto-Rheological Fluid, <https://www.lord.com>.